Supplementary Information for

All-Polymer Heterojunction Nanoparticles Enable Reproducible and Enhanced Hydrogen Evolution Photocatalysis

Charles Jeffreys[1], Yakun He[1], Nisreen Alshehri[1,2], Lingyun Zhao[3], Adam V. Marsh[1], George T. Harrison[1], Oleksandr Matiash[1], Aren Yazmaciyan[1,4], Christopher E. Petoukhoff[1], Shadi Fatayer[1], Frédéric Laquai[1,5], Martin Heeney[1,6]*

[1] Physical Science and Engineering Division, King Abdullah University of Science and Technology (KAUST), Thuwal 23955-6900, Kingdom of Saudi Arabia.

[2] Physics and Astronomy Department, College of Sciences, King Saud University, Riyadh 12372, Kingdom of Saudi Arabia.

[3] KAUST Core Labs, King Abdullah University of Science and Technology (KAUST), Thuwal, Kingdom of Saudi Arabia.

[4] Paul Drude Institute for Solid State Electronics, Hausvogteiplatz 5-7, Berlin 10117, Germany.

[5] Chair of Physical Chemistry and Spectroscopy of Energy Materials, Department of Chemistry, Ludwig-Maximilians-Universität München, Munich 81377, Germany.

[6] Department of Chemistry and Centre for Processable Electronics, Imperial College London, White City Campus, London, W12 0BZ, UK.

Table of Contents

Experimental

Materials:
PM6 was purchased from Thermo Fischer Scientific, PJ1-R was purchased from eFlex and Y6 was purchased from 1Material. TEBS was purchased from Solaris Chem. Water came directly from a Milli-Q distillery. All materials and solvents were used without further purification or filtration.

Nanoparticle Fabrication:
Stock solutions of PM6, Y6, and PJ1-R (0.5 mg mL^{-1}) were prepared in chloroform. The solutions were heated to 40˚C and stirred overnight to ensure complete dissolution. The PM6 and either PJ1-R or Y6 stock solutions were mixed in the desired ratio to give a 5 mL mixed solution. The mixed solution was stirred for 30 mins to ensure even distribution of materials and then added to 10 mL of aqueous TEBS solution (0.5 wt%). To form a pre-emulsion, the suspension was stirred at 1500 rpm at 40 ˚C for 30 minutes, then immediately was sonicated for 5 minutes (Sonics VibraCell VCX130PB at 77% power). To remove the chloroform, the samples were immediately stirred at 400 rpm, heated to 80˚C, and placed under a gentle stream of nitrogen. The resulting NP solution was used directly without any further purification.

Dynamic Light Scattering:
Each nanoparticle sample's size distribution was determined by dynamic light scattering using Malvern Zetasizer ZS. A sample of nanoparticle was diluted by a factor of 100 and placed in a 1cm cuvette. The average of 3 scans was used for each distribution.

Hydrogen Evolution Reaction (HER) Measurements:
HER rates of PM6:PJ1-R NPs were measured using ascorbic acid as a sacrificial hole scavenger. A given nanoparticle sample (2.3-2.4 mg approx., mass quantified according to UV-VIS spectroscopy) was loaded into a 12 mL rectangular prism reactor cell with a square face of surface area of 4.4 ± 0.1 cm^{-2}. Ascorbic acid (422.69 mg) was added, and the solution (0.2 M) was made up to 12 mL. The required amount of platinum was loaded by adding a specific volume of aqueous potassium hexachloroplatinate solution (0.401 mg mL^{-1} Pt), and photo-depositing in-situ under a 300 W Xe Lamp (Asahi Max 303) fitted with an ultraviolet-infrared mirror module (240-1100 nm). The light intensity was set to 1 sun using a calibrated spectrometer (Ocean Optics USB2000 calibrated with an Ocean Optics DH3-plus light source) fitted with a fibre optic cable and a 0.4778-cm^2 cosine corrector. The reactor was purged 10x with inert argon (never taking pressure below 100 Torr to avoid water evaporation in the sample), and the reaction pressure was set to 100 Torr. The amount of hydrogen was quantified by thermal conductivity detector in a calibrated gas chromatograph, using a standard reference gas mixture to determine integration area.

UV-VIS Spectroscopy:
UV-VIS spectra were acquired using an Ocean Insight High Resolution Spectrometer, connected to a DH-2000-BAL light source using 600 μm SR fibres with a Square One cuvette holder. A 3% neutral density filter was placed after cuvette illumination as to not saturate the spectrometer. Samples were prepared from a stock solution of nanoparticles with an accurately measured concentration. Then serial dilutions were made by adding the appropriate volume of Milli-Q water.

Photoluminescence Spectroscopy:
Nanoparticle samples were made according to the mini emulsion method outlined previously, with no Pt photodeposition. Neat PM6, neat PJ1-R, and blend sample (7:3) suspensions were made in water at 125 μg mL^{-1} concentrations. Measurements were carried out on a Jobin Yvon Fluorolog spectrofluorometer from Horiba. Samples were placed in a quartz cuvette, excited using a Xe lamp and detected using either a R928 PMT detector (neat PM6), or an InGaAs array detector (neat PJ1-R and 7:3 blend). Neat PM6 measurements were conducted by excitation at 600 nm with a grating of 1200 gr mm^{-1}, whilst neat PJ1-R and 7:3 blend samples were excited at 730 nm with a grating of 600 gr mm^{-1}.

Transient Absorption Spectroscopy (TAS):
TAS was carried out using a home-built pump-probe setup. The output of a Ti:sapphire amplifier (Coherent LEGEND DUO, 800 nm, 4.5 mJ, 3 kHz, 100 fs) was split into four beams (2 mJ, 1 mJ, 1 mJ, and 0.5 mJ). The three higher energy beams were used to separately pump three optical parametric amplifiers (OPA; Light Conversion TOPAS Prime). One of the 1 mJ TOPAS generated wavelength-tuneable pump pulses (240-2600 nm, using Light Conversion NIRUVIS extension). A fraction of the 0.5 mJ output of the Ti:sapphire amplifier was focused into a c-cut 3 mm thick sapphire window, thereby generating a white light supercontinuum from 500 to 1800 nm. Pump and probe beams were focused on the sample to spot sizes of 1.0 mm and 0.1 mm diameter, respectively (from a Gaussian fit at 86.5% intensity), as measured using a beam profiler (Coherent LaserCam-HR II). The transmitted fraction of the white light was guided to a custom-made prism spectrograph (Entwicklungsbüro Stresing) where it was dispersed by a prism onto a 512-pixel CMOS linear image sensor (Hamamatsu G11608-512A).

For ps-ns dynamics, the pump-probe delay time was achieved by varying the probe path length using a broadband retroreflector mounted on a 600 mm automated mechanical delay stage (Thorlabs optical delay line ODL600/M), generating delays from -500 ps to 7.5 ns. The pump was mechanically chopped to a repetition rate of 1.5 kHz. For ns-ms dynamics, the pump pulse was provided by an actively Q-switched Nd:YVO_4 laser (InnoLas Picolo-AOT 1-MOPA, 1064 nm, 2.5 W, 5 kHz, <0.8 ps) frequency-doubled, providing pulses at 532 nm. The pump laser was triggered by an electronic delay generator (Stanford Research Systems DG535) itself triggered by the transistor–transistor logic sync from the Legend DUO, allowing control of the delay between pump and probe with a jitter of roughly 100 ps. The trigger frequency from the Legend DUO was reduced by 2 to give the excitation pulse repetition rate of 1.5 kHz to obtain the pump-on and pump-off signals.

The probe pulse repetition rate and detector array readout rate were 3 kHz. Adjacent diode readings corresponding to the transmission of the sample after excitation and in the absence of an excitation pulse were used to calculate ΔT/T. Measurements were averaged over several thousand shots to obtain a good signal-to-noise ratio. The chirp induced by the transmissive optics was corrected with a home-built Matlab code.
The nanoparticle dispersions were prepared to have an OD of 0.2 at 530 nm (i.e., 66.7 μg/mL for PM6; 83.7 μg/mL for PJ1-R; 71 μg/mL for PM6:PJ1-R), then were loaded into a 1 mm quartz cuvette for the measurements. The same samples were used for both TA and TRPL measurements.

Time-Resolved Photoluminescence Spectroscopy (TRPL):
TRPL spectroscopy was carried out using a free-space coupled streak camera setup. The output of a wavelength-tunable Ti:sapphire oscillator laser (Coherent CHAMELEON ULTRA I, 690-1040 nm, 2.9 W, 80 MHz, 140 fs), tuned to 1000 nm, was directed into an optical parametric oscillator (Coherent Compact OPO), for second harmonic generation to achieve 500 nm. The 500 nm excitation beam was guided to the sample and was incident on the 1 mm cuvette with a spot size of 1.5 mm. The photoluminescence (PL) of the samples was collected by an optical telescope (consisting of two plano-convex lenses), focused onto the slit of a spectrograph (Princeton Instruments Acton Spectra Pro SP2300), and detected with a streak camera (Hamamatsu C10910) system. An 80.2 MHz synchroscan unit (Hamamatsu M10911-01) was used to measure the picosecond dynamics. Laser excitation was filtered out using a 550 nm long pass filter. The data was acquired in photon counting mode using the streak camera software (HPDTA).
Two separate time ranges were used: time range 5 for the neat films (maximum time range of 2 ns), and time range 3 for the blends (maximum time range of 500 ps). The instrument response function (IRF) of the system, measured by collecting the scattered laser light from the sample, was 32.5 ps for time range 5, and 7.84 ps for time range 3.

Absolute Photoluminescence Quantum Yield (PLQY):
Absolute intensity-calibrated PLQY measurements were carried out using a home-built system. Excitation for the PL measurements was performed using a continuous wave (CW) laser (Hübner Photonics Cobolt 06-MLD diode laser series) through an optical fiber into a 4-inch integrating sphere (Labsphere). The spot size was adjusted using a beam collimator on the output of the fiber to be 2.67 mm in diameter. The sample angle was fixed at ~5° off-normal incidence, angled towards the exit port. A second optical fiber was used from the output of the integrating sphere (90° from the input port) to a fiber-coupled filter mount, where neutral density (ND) or long-pass (LP) filters could be installed. A third optical fiber was used to couple light from the filter mount to either the visible (Avantes AvaSpec-ULS2048XL-EVO) or NIR detectors (custom Entwicklungsbüro Stresing detector, composed of a Princeton Instruments Acton SP-2-150i spectrograph, with a grating having 150 grooves/mm and 1.2 mm blaze, and a Hamamatsu G11608 InGaAs linear image sensor). The system was calibrated at each central wavelength by using a calibrated Halogen light source (Ocean Optics HL-3 plus) with specified spectral irradiance, which was connected directly to the integrating sphere. The measured irradiance of the calibration lamp was used to construct a correction file, in units of photons/(nm·count), which was then applied to the measured spectra from the samples.

Measurements: To obtain the PLQY, the following measurements were conducted: 1) sample emission (Em_{sample}); 2) sample excitation (Ex_{sample}); 3) sphere emission (Em_{sphere}); and 4) sphere excitation (Ex_{sphere}). The PLQY was then determined by the following equation, after performing the absolute-intensity correction to each of the measured spectra and integrating over the full emission or excitation wavelength ranges:

$$\text{PLQY} = \frac{\#\text{ photons emitted}}{\#\text{ photons absorbed}} = \frac{Em_{sample} - Em_{sphere}}{Ex_{sample} - Ex_{sphere}} \quad Equation\ 1$$

All measurements used the same integration time and number of accumulations: 1000 ms × 10 for PM6; 100 ms × 100 for PJ1-R. Emission measurements were conducted with a 550 nm LP filter installed for PM6; excitation measurements were conducted with an OD 3 ND filter for PM6. These were not required for measurements in the NIR due to the lower sensitivity to the excitation wavelength. The excitation wavelength and power were 515 nm and 29.5 mW for PM6, and 660 nm and 3.94 mW for PJ1-R. The nanoparticle dispersions were prepared to have an OD of 0.28 at 530 nm (i.e., 93 μg/mL for PM6; 117 μg/mL for PJ1-R), then were loaded into a 1 mm quartz cuvette for the measurements. A water-filled cuvette was used as a blank for the empty sphere measurements.

Cryo-TEM Specimen Preparation and Data Acquisition:
Cryo-TEM specimens were prepared using a Vitrobot Mark IV automated plunge-freezing system (Thermo Fisher Scientific). C-flat holey carbon grids (R 1.2/1.3, 300 mesh, copper) were glow-discharged prior to use. A 3 μL aliquot of the nanoparticle dispersion was applied to the grid, blotted for 3 seconds, and plunge-frozen into liquid ethane cooled by liquid nitrogen. All subsequent grid handling and transfer were performed under cryogenic conditions (liquid nitrogen temperature). Samples containing only PM6 or only PJ1-R were imaged on a Titan Krios G4 cryo-TEM (Thermo Fisher Scientific) operated at 300 kV, equipped with a Selectris energy filter and Falcon 4i direct electron detector. Images were acquired in energy-filtered transmission electron microscopy (EFTEM) mode at a nominal magnification of 130,000× (calibrated pixel size of 0.93 Å at the specimen level) with a total electron dose of 50 $e^-/Å^2$ using Velox software (version 3.18). The PM6:PJ1-R complex sample was imaged on a Titan Krios G2 cryo-TEM (Thermo Fisher Scientific) operated at 300 kV, equipped with a Gatan GIF Quantum 968 energy filter and a Gatan K2 Summit direct electron detector. Images were recorded in dose-fractionated mode in EFTEM at a nominal magnification of 130,000× (calibrated pixel size of 1.06 Å at the specimen level) with a total electron dose of ~50 $e^-/Å^2$ using Gatan DigitalMicrograph software (version 3.2). All cryo-TEM images were processed and analysed using Fiji (ImageJ version 2.16.0).

Pt cluster particle distribution analysis:
Raw files of the cryo-TEM were loaded into FIJI (ImageJ) (software version 2.16.0). A scale was set to 9.2523814 pixels/ nm and the image contrast was adjusted to make prominent the dark clusters of the nanoparticle. To reduce noise, a Gaussian blur filter was applied with 0.5 nm radius. A threshold mask was set to identify the darkest parts of the image until all clusters were highlighted, then the 'analyse particles' tool was used to identify objects with 0.7-1.0 circularity (to eliminate rod structures from the lamella stacks), and an area of >1.5 nm^2. The areas for each cluster were assumed to be circular, and equation 2 gave the diameter:

$$D = 2\sqrt{\frac{area}{\pi}} \quad Equation\ 2$$

Photoelectron and inverse photoelectron measurements:
Samples were prepared on 200 nm metallic substrates of Au sputtered onto clean polished silicon. The thin organic films were prepared by spin coating at 5 mg/ml concentration at 4000-5000 revolutions per minute in a fume hood and then mounted on Omicron style sample plates with good electrical contact to the plate made with Mo strips. Ultraviolet photoelectron (UPS) measurements were performed in a UHV chamber (ScientaOmicron) operating at a pressure of 5×10^{-10} mbar. This was equipped with a 21.2 eV vacuum ultraviolet source (VUV) (focus). A 1486.7 eV Al Kα monochromatic X-ray source (XM1000) was used for XPS. Measurements were performed without charge compensation in electrical contact to the analyser. The sample was biased by 10 eV to observe the low kinetic energy cutoff in UPS. The electron analyser was an Argus CU. Measurements were conducted with an X-ray source-Analyser angle of 80 ° and electron take off angle of 0° (normal to sample plane) for both XPS and UPS. UPS was conducted with an attenuation reducer, a copper plate with a small aperture to reduce intensity and mitigate sample damage and charging. IPES was conducted in an adjacent home-built chamber consisting of an electron source (Staib) operating at 20-30 eV with an energy dispersion of 0.25 eV directed normal to the sample. The sample was biased to be 20 eV. The resulting inverse photo-emission was detected through a focusing assembly consisting of an arrangement of two focusing lens (one vacuum, one air side) and an air side photo-multiplier tube (PMT) (Hamamatsu). All extraneous light was eliminated during measurements by covering port windows and sealing the detector.

Calculation of exciton diffusion length in PJ1-R

Following a pulsed excitation, the exciton density (n_{exc}) decays by a combination of their return to the ground state [i.e. intrinsic lifetime (τ)] and bimolecular SSA[51] as represented in the following rate-equation (Equation 3):

$$\frac{dn_{exc}}{dt} = -\frac{n_{exc}}{\tau} - \frac{\alpha}{2} n_{exc}^2$$

where α is the bimolecular SSA rate constant which is related to the excitons diffusion coefficient D (considering a three-dimensional diffusion model)[51] as follows (Equation 4):

$$D = \alpha / (8\pi R_a)$$

where R_a is the singlet exciton annihilation radius. From there, the exciton diffusion length is obtained as (Equation 5):

$$L_D = \sqrt{D\tau}$$

The singlet exciton decay following a pulsed excitation is described by Equation 2 which has the following analytical solution for an initial exciton density n_0 (Equation 6):

$$n(t) = \frac{n_0 e^{-t/\tau}}{1 + \alpha\tau / 2\, n_0 \left[1 - e^{-t/\tau}\right]}$$

From the SSA rate constant α, the exciton diffusion coefficient D is calculated using Equation (3), considering an exciton annihilation radius (R_a) of 1 nm.

	Mn	Mw	Polydispersity
PM6	29k	65k	2.26
PJ1-R	8.6k	12.4k	1.44

Supplementary Table 1 – High Temperature GPC data for molecular weight of PM6 and PJ1-R polymers, measured in 1,2,4-trichlorobenzene solvent at 150˚C, against narrow dispersity polystyrene standards.

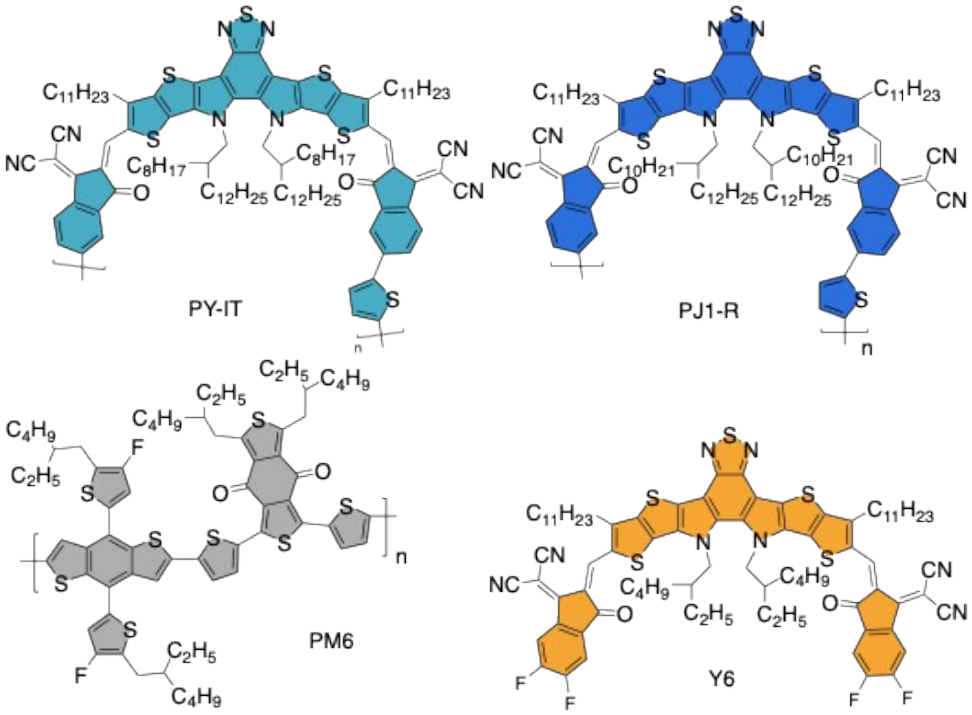

Supplementary Figure S1 – Structures of PY-IT, PJ1-R, PM6, and Y6.

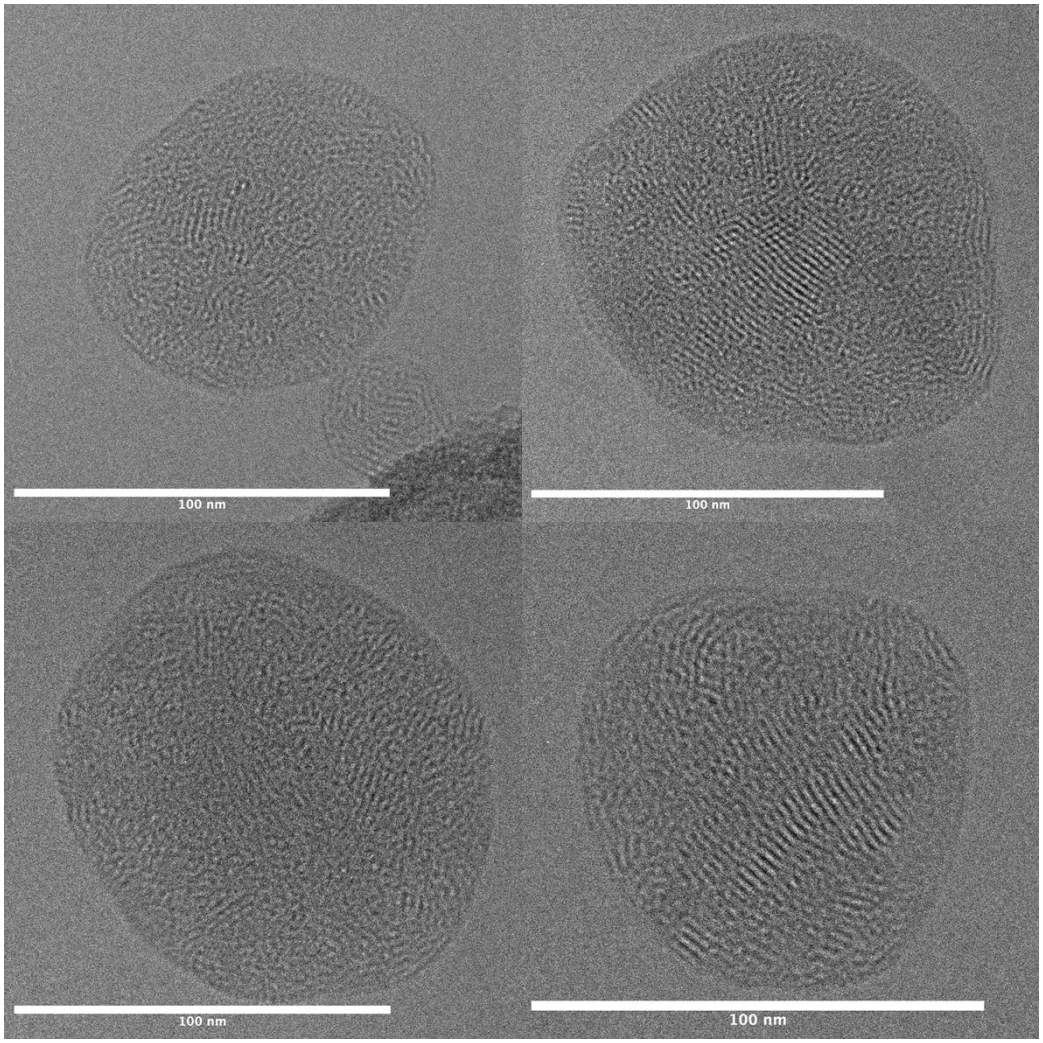

Supplementary Figure S2 – Cryo TEM images of PM6:Y6 nanoparticles, stabilised by TEBS surfactant.

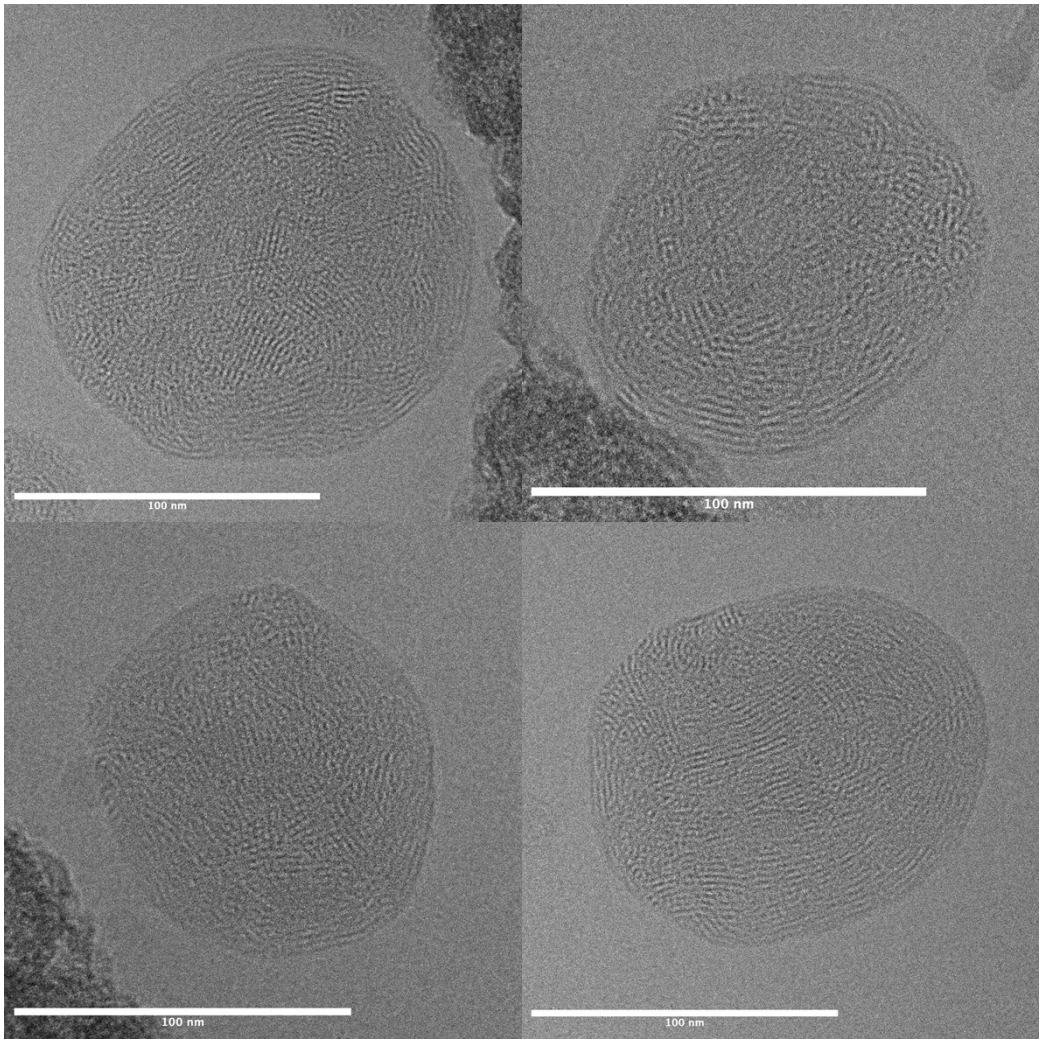

Supplementary Figure S3 – CryoTEM images of PM6:PJ1-R stabilised by TEBS Surfactant.

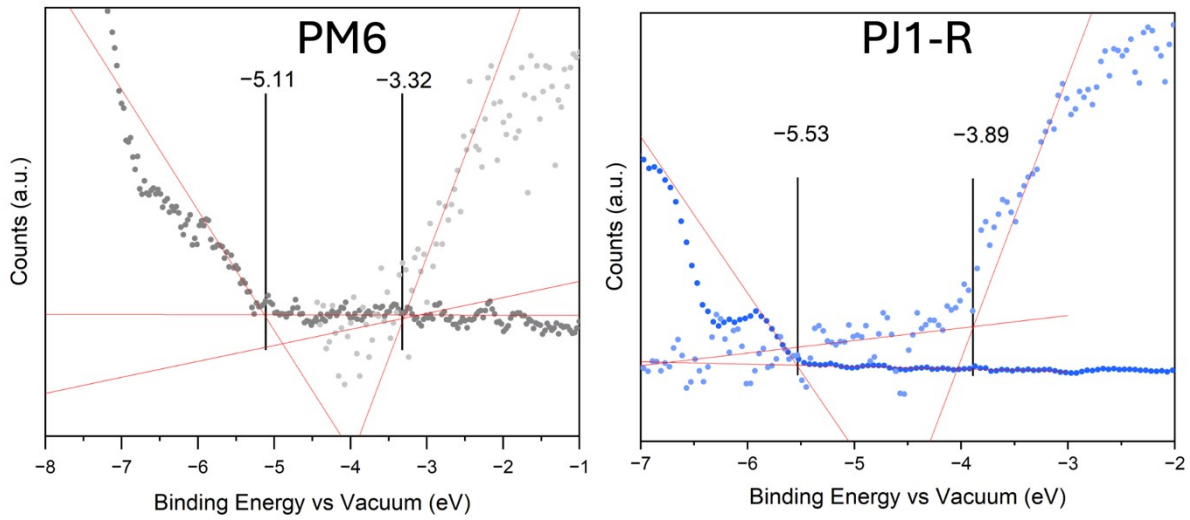

Supplementary Figure S4 - UPS-IPES spectra for PM6 (left) and PJ1-R (right) against vacuum.

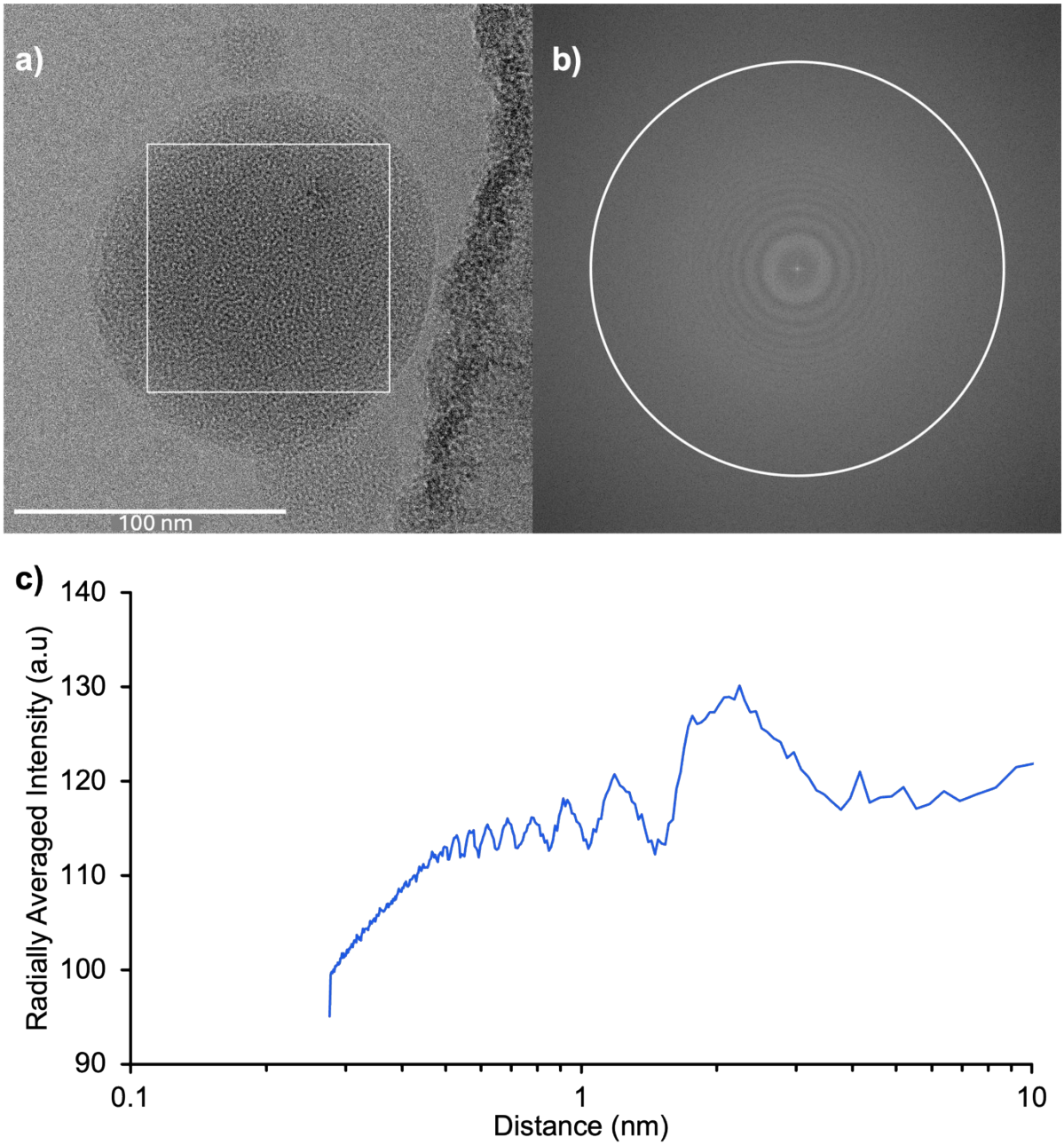

Supplementary Figure S5 – a) High resolution cryo-TEM image of a neat PJ1-R nanoparticle, with white box showing area of FFT analysis. b) FFT profile of nanoparticle, with white circle indicating the area of a radial plot profile, averaging intensities in concentric rings of increasing radius. c) Radially averaged intensity profile from the FFT of a high-resolution TEM image of the sample. Intensity values are averaged across concentric rings originating from the FFT centre, revealing characteristic spatial frequencies corresponding to lamellar spacing in the nanostructure. Major peak at ~2.3 nm is taken as this sample's packing distance. Average packing distances were calculated by averaging 25 nanoparticle images using this methodology to give a mean of 2.1 ± 0.17 nm.

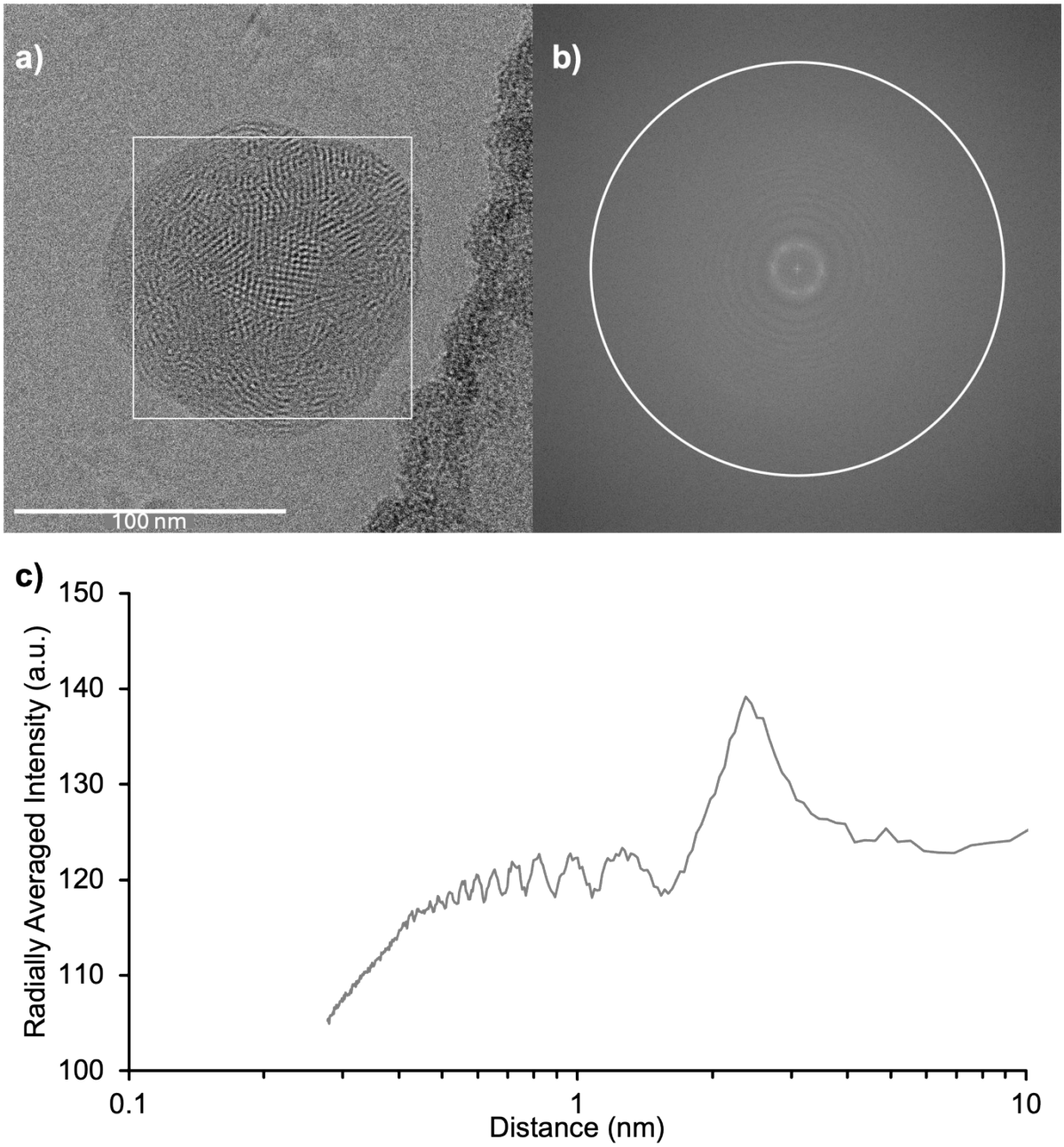

Supplementary Figure S6 – a) High resolution cryo-TEM image of a neat PM6 nanoparticle, with white box showing area of FFT analysis. b) FFT profile of nanoparticle, with white circle indicating the area of a radial plot profile, averaging intensities in concentric rings of increasing radius. c) Radially averaged intensity profile from the FFT of a high-resolution TEM image of the sample. Intensity values are averaged across concentric rings originating from the FFT centre, revealing characteristic spatial frequencies corresponding to lamellar spacing in the nanostructure. Major peak at ~2.4 nm is taken as this sample's packing distance. Average packing distances were calculated by averaging 25 nanoparticle images using this methodology to give a mean of 2.41 ± 0.07 nm.

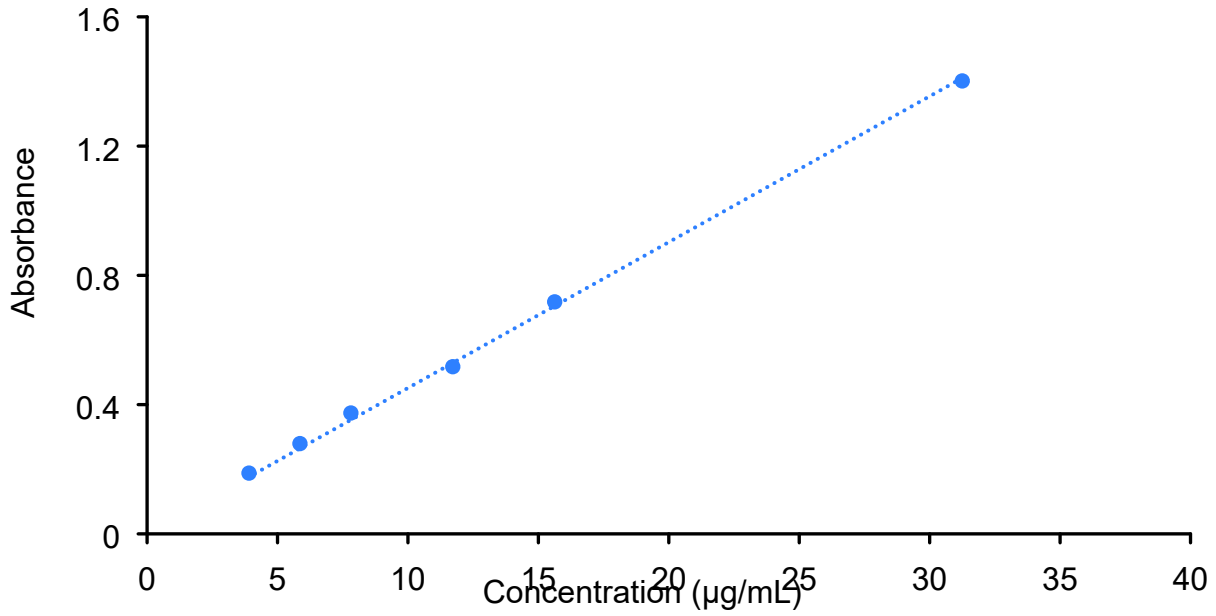

Supplementary Figure S7 – Absorbance vs. concentration graph for neat PJ1-R nanoparticles for calculation of the extinction coefficient at 795 nm.

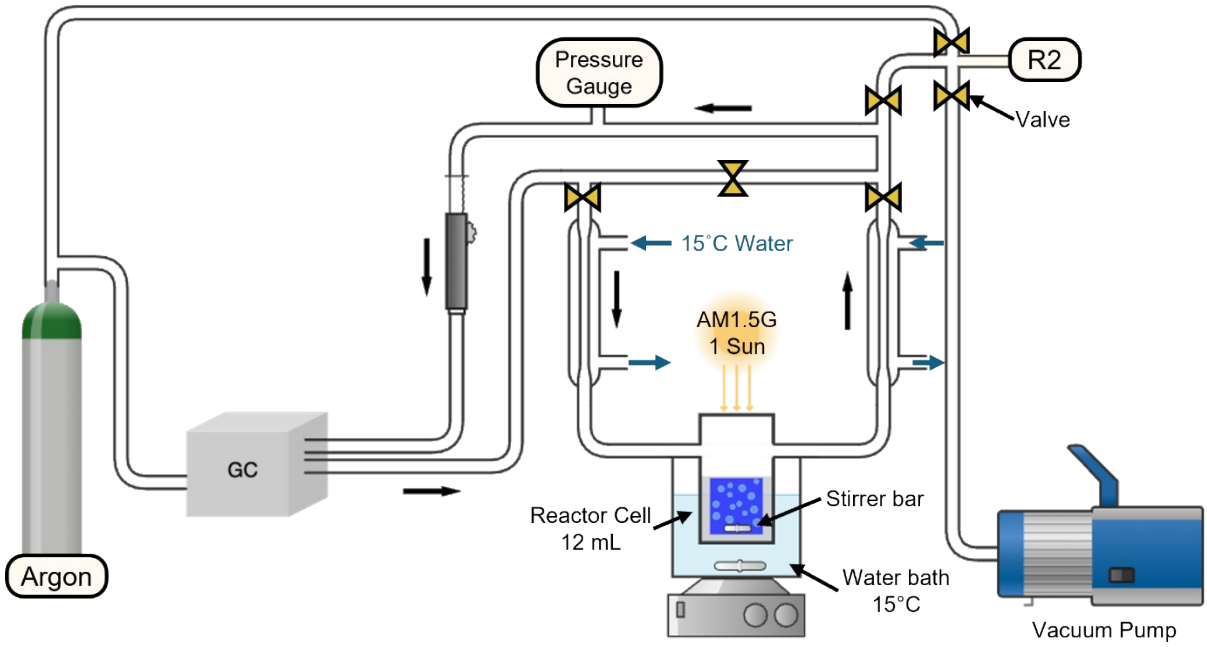

Supplementary Figure S8 – Schematic diagram of hydrogen evolution reactor used for photocatalytic performance measurements.

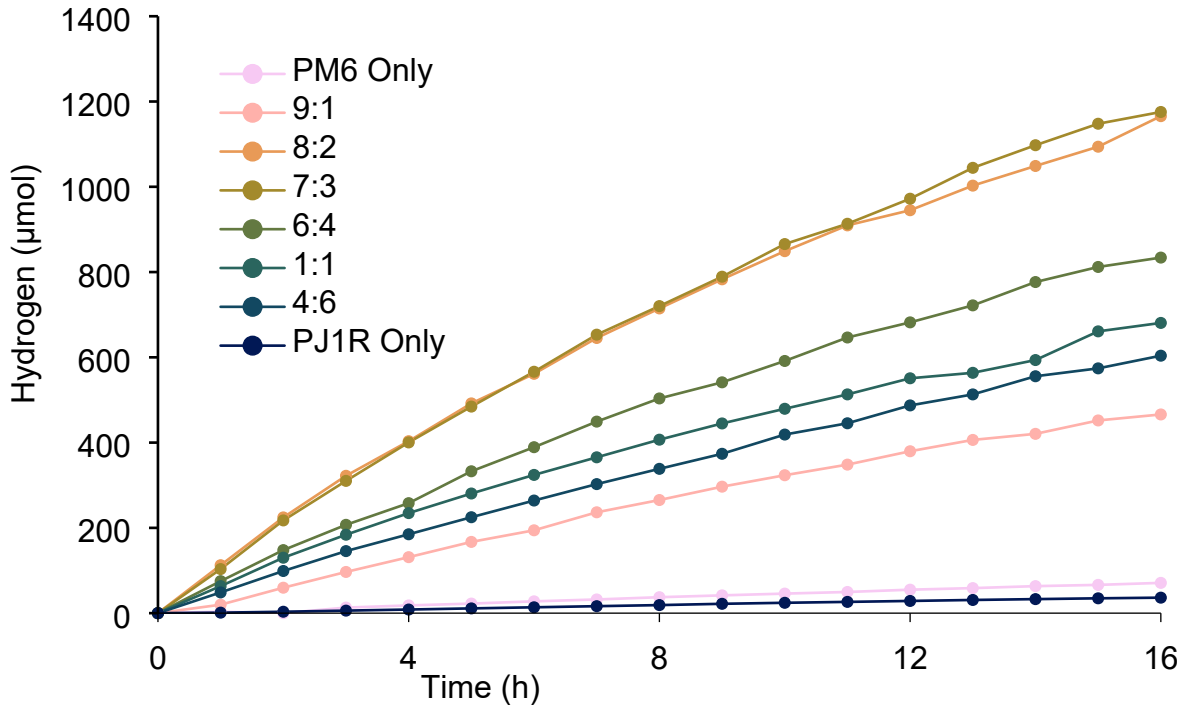

Supplementary Figure S9 – Hydrogen produced over time across varying donor-acceptor ratios with 10% Pt loading.

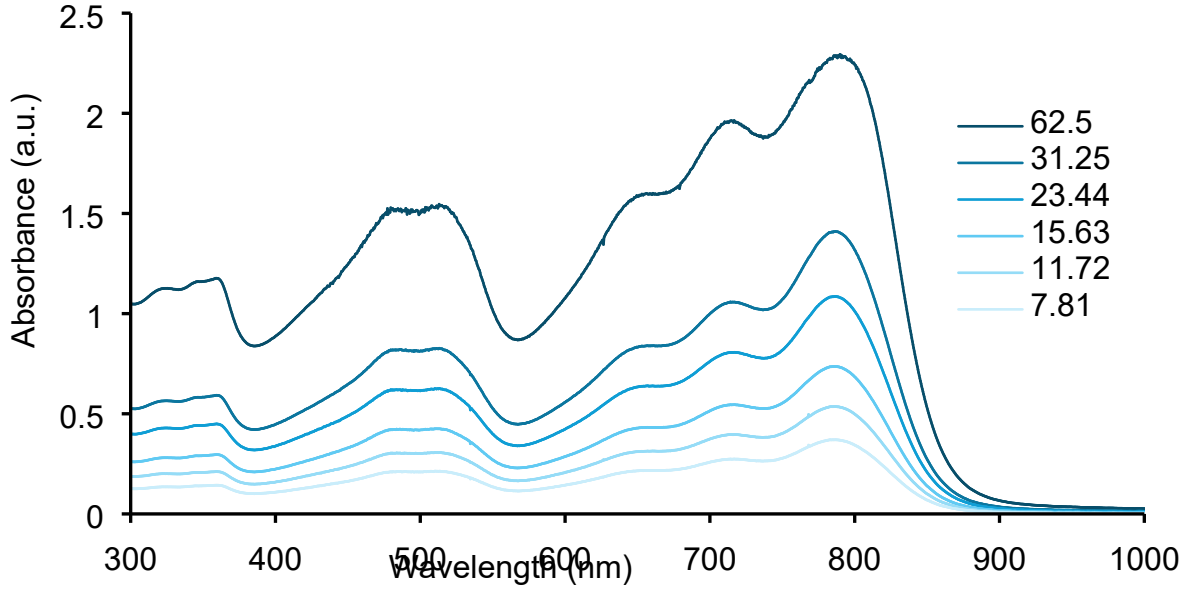

Supplementary Figure S10 – UV-Vis absorbance spectrum of neat PJ1-R nanoparticles at different concentrations (µg/mL).

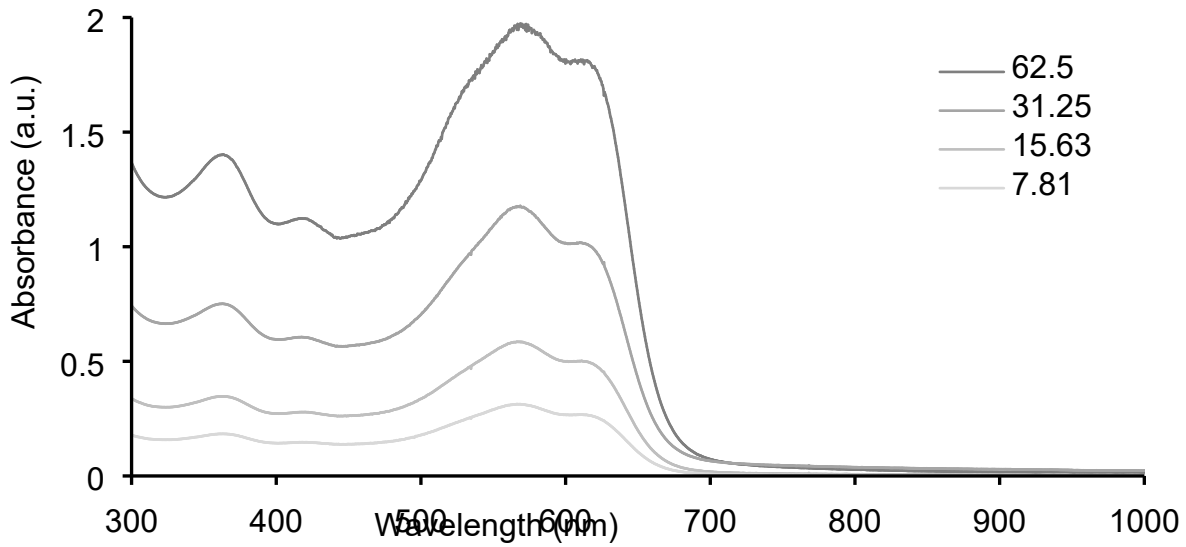

Supplementary Figure S11 – UV-Vis absorbance spectrum of neat PM6 NPs at different concentrations (µg/mL).

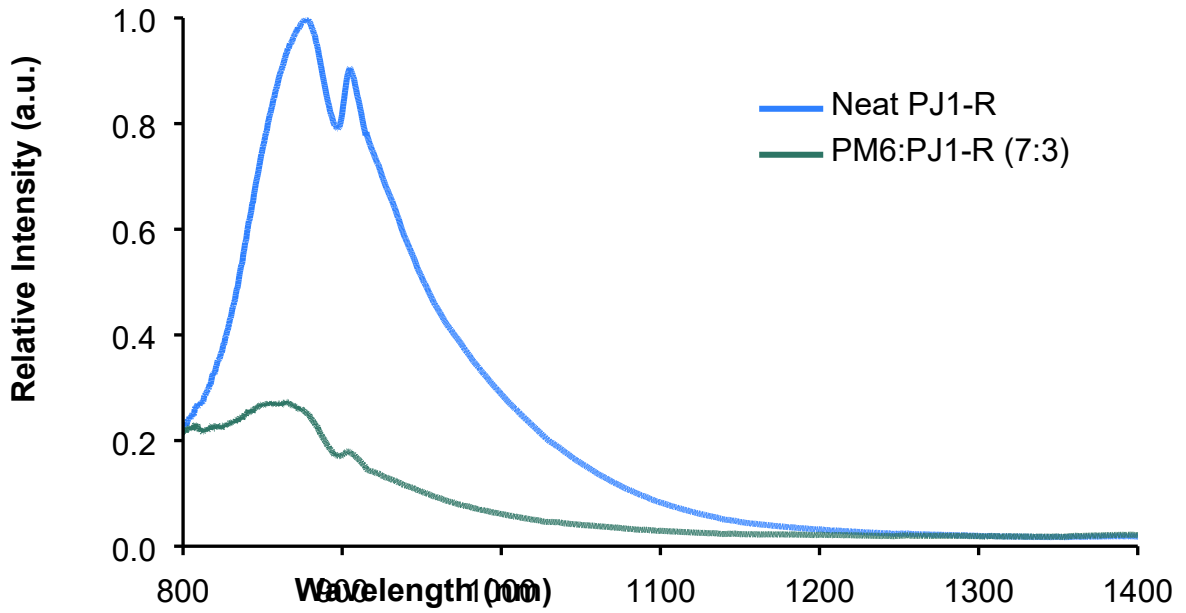

Supplementary Figure S12 – Photoluminescence spectra for neat PJ1-R NPs and PM6/PJ1-R (7:3) blend nanoparticles, intensity values for both neat and blend samples divided by the counts value of the neat PJ1-R peak at 880 nm. Note: the detector used for these measurements has a characteristic drop in intensity at 900 nm which is observed in all measurements – it is not characteristic of the materials used in this study.

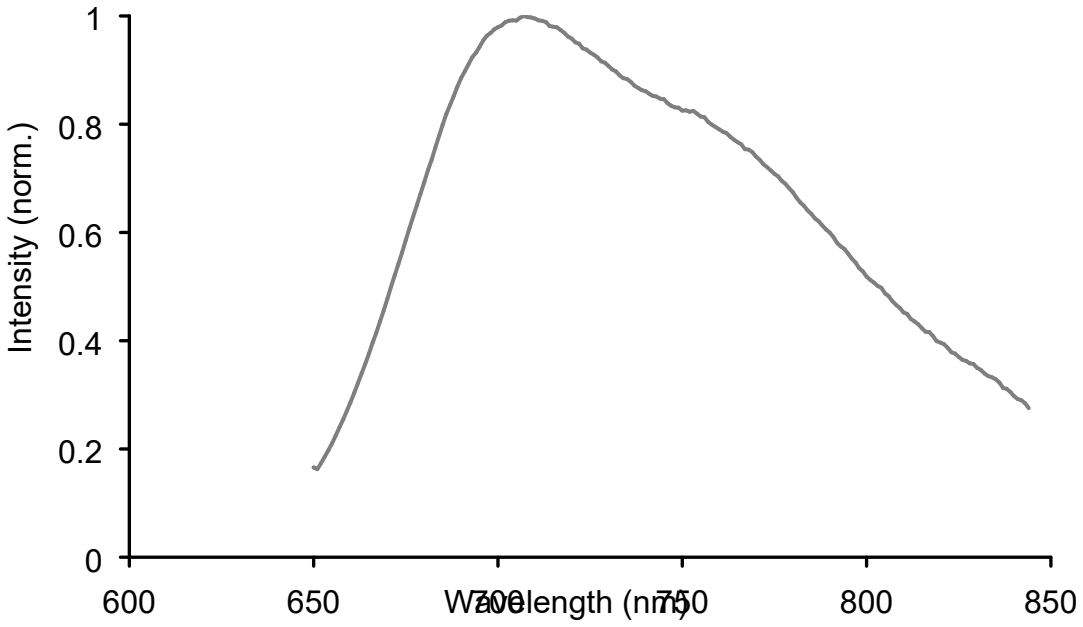

Supplementary Figure S13 – Normalised photoluminescence emission spectrum for neat PM6 nanoparticles.

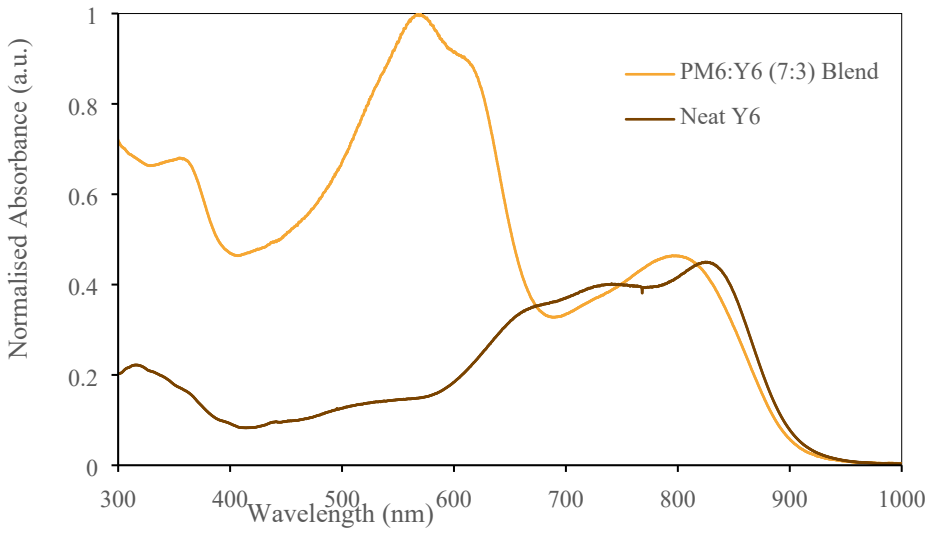

Supplementary Figure S14 – Normalised absorbance spectrum for optimised PM6:Y6 (7:3) and neat Y6 nanoparticles.

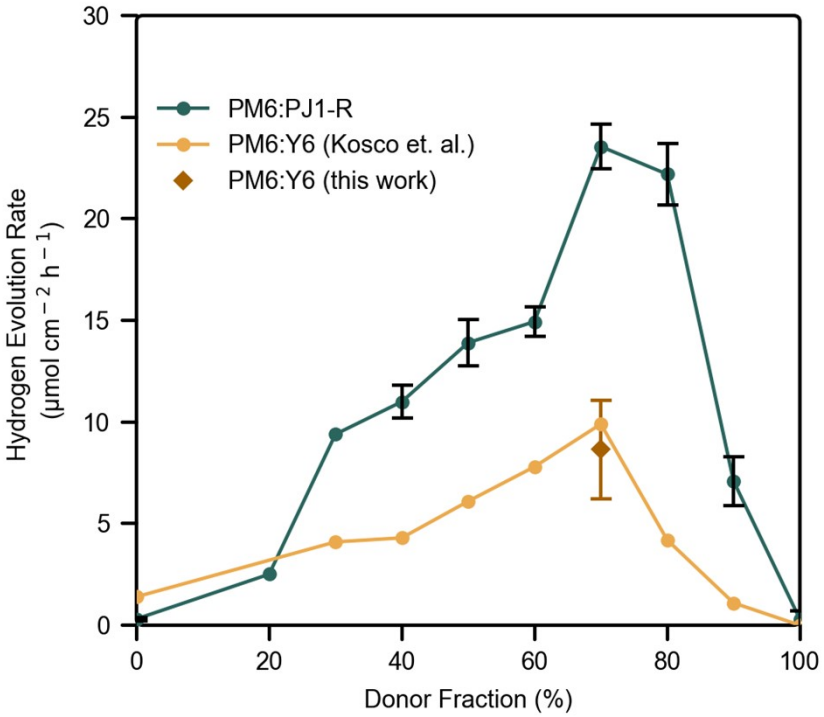

Supplementary Figure S15 – Donor: acceptor ratio optimisation for PM6:PJ1-R nanoparticles, as well as the measured rates of PM6:Y6 from this study. The values are compared to reported data from Kosco et al.[21]

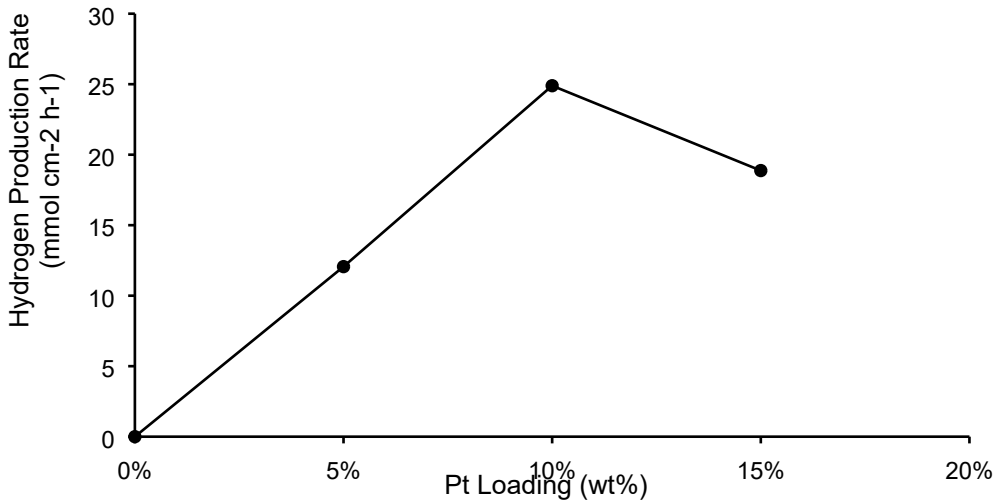

Supplementary Figure S16 – Hydrogen Evolution rate of PM6:PJ1-R (7:3) nanoparticles with varying Pt loading, using sacrificial AA and 1 sun illumination intensity.

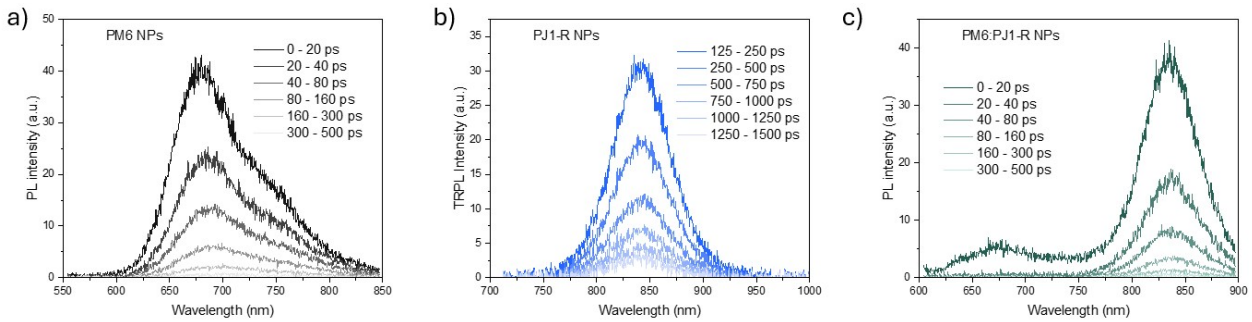

Supplementary Figure S17 – PL intensities of (a) neat PM6, (b) neat PJ1-R, and (c) PM6:PJ1-R blend nanoparticles as a function of decay time with an excitation wavelength of 500 nm.

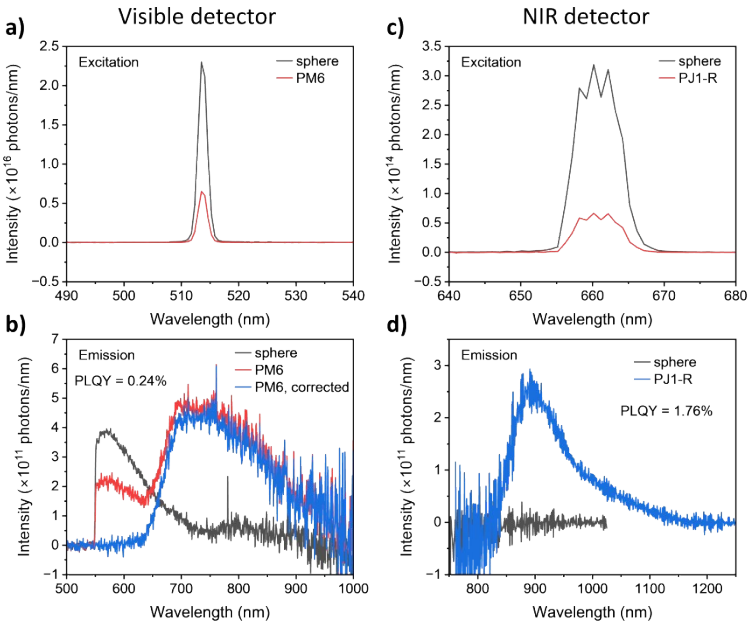

Supplementary Figure S18 – Absolute-intensity calibrated excitation (a,c) and emission (b,d) spectra used for PLQY calculations for a,b) PM6 and c,d) PJ1-R. For PM6, residual laser excitation was present in the emission measurement (b), which was removed by scaling the sphere emission to the PM6 emission in the range of 555-600 nm, then subsequently subtracting it. There was no residual laser excitation present in the PJ1-R emission spectra (d) due to the lower sensitivity of the NIR detector to 660 nm wavelengths. Using the photoluminescence quantum yield (PLQY) of 1.76% for PJ1-R and 0.24% for PM6, the radiative lifetime can be determined to be 25.5 ns and 41.5 ns for PJ1-R and PM6, respectively.

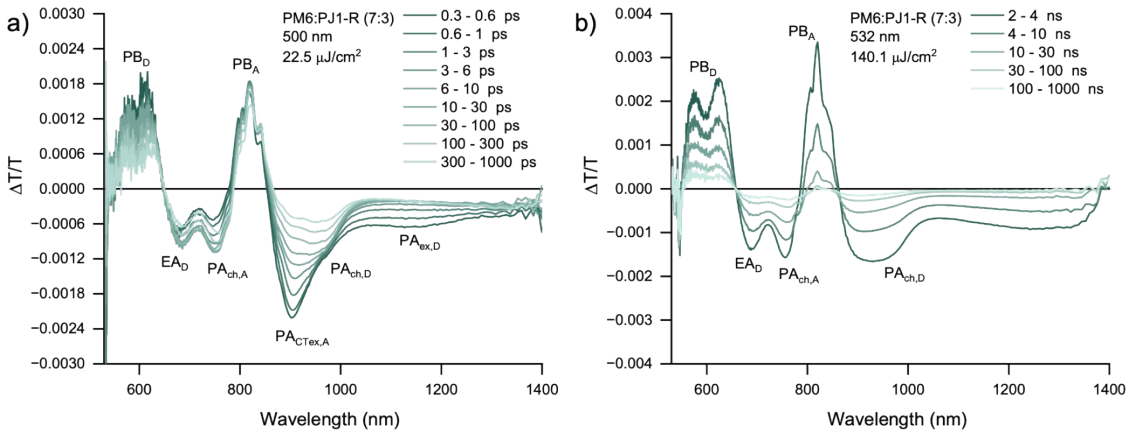

Supplementary Figure S19 – a) short delay TA spectra for PM6:PJ1-R (7:3) nanoparticles excited at 500 nm and b) long delay TA spectra excited at 532 nm.

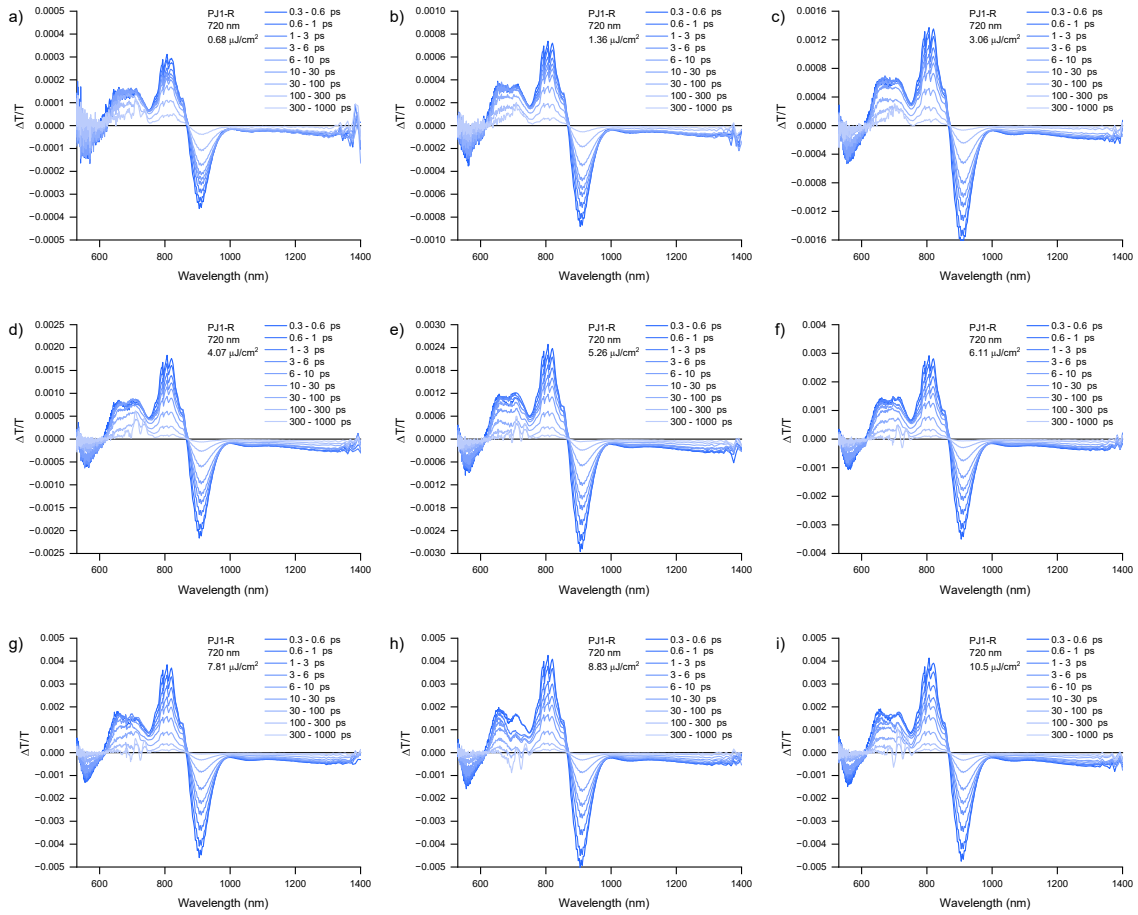

Supplementary Figure S20 – Fluence dependency of TA spectra of neat PJ1-R nanoparticles at 720 nm excitation. High noise from 650 – 780 nm was due to scattering. Photoinduced absorption at 880-895 nm was used for calculation of exciton diffusion length.

References:

(21) Kosco, J.; Gonzalez-Carrero, S.; Howells, C. T.; Fei, T.; Dong, Y.; Sougrat, R.; Harrison, G. T.; Firdaus, Y.; Sheelamanthula, R.; Purushothaman, B.; Moruzzi, F.; Xu, W.; Zhao, L.; Basu, A.; De Wolf, S.; Anthopoulos, T. D.; Durrant, J. R.; McCulloch, I. Generation of Long-Lived Charges in Organic Semiconductor Heterojunction Nanoparticles for Efficient Photocatalytic Hydrogen Evolution. *Nat. Energy* **2022**, *7* (4), 340–351. https://doi.org/10.1038/s41560-022-00990-2.

(51) Yang, W.; Pursglove De Castro, C. S.; Karuthedath, S.; Firdaus, Y.; Alshehri, N.; Chen, S.; Rosas Villalva, D.; Petoukhoff, C. E.; Dahman, A.; Baran, D.; Anthopoulos, T. D.; Laquai, F.; Gorenflot, J. Determining Exciton Diffusion Length in Organic Semiconductors: Unifying Macro- and Microscopic Perspectives. *Adv. Energy Mater.* **2025**, 2405322. https://doi.org/10.1002/aenm.202405322.